

## **Absorbing microspheres in water : laser radiation pressure and hydrodynamic forces**

**Rumiana Dimova<sup>1,2</sup> and Bernard Pouligny<sup>1</sup>**

<sup>1</sup>Centre de recherche Paul-Pascal, CNRS, av. A. Schweitzer, 33600 Pessac, France

<sup>2</sup>Laboratory of Thermodynamics and Physico-Chemical Hydrodynamics, Faculty of Chemistry, University of Sofia, 1126 Sofia, Bulgaria

### **Abstract**

We show examples of optical levitation and trapping of micron-sized particles in water. Experiments use a long-working-distance optical trap made of vertical counter propagating laser beams, in Gaussian or tubular (TEM<sub>01</sub>\*-like) modes. This configuration allows us to separate radiation pressure (RP) forces from those due to thermal convection. RP forces are found dominant with bare polystyrene particles and in quantitative agreement with those computed with the Generalized Lorenz-Mie Theory (GLMT). In the case of strongly absorbing magnetic particles, thermal effects are found dominant whenever the power intercepted by the trapped particle exceeds a milliwatt. The absorption of such particles is estimated using GLMT from the extrapolated zero-power levitation intensity.

### **1) Introduction**

Radiation pressure (RP) is the direct manifestation of the momentum conveyed by an

electromagnetic wave. A laser beam illuminating a particle creates a RP force on the order of  $\Phi/c$  : here  $\Phi$  is the power intercepted by the particle and  $c$  is the velocity of light. Thus a milliwatt produces a few piconewtons, which is enough to equilibrate the weight of a particle a few micrometers in size.

Levitation of particles by laser beams was first demonstrated in the early seventies<sup>[1] [2]</sup> with moderately focussed laser beams and spherical particles. Not only levitation, but also stable 3-dimensional (3d) trapping was demonstrated in geometries using 2 counter-propagating beams<sup>[1] [2]</sup>.

2-beam geometries are delicate and not universal, because the appropriate size and separation of the beam-waists depend on the size and refractive index of the particle to be trapped<sup>[2]</sup>. Interestingly, 3d optical trapping can be achieved very simply by means of a single tightly focussed beam, a geometry known as the “optical tweezers”<sup>[3] [4]</sup>. Apparently, single-beam traps work with particles of very different sizes, although reasons for this universality are not clear<sup>[5]</sup>.

Optical trapping -whatever the geometry- yields the possibility of holding and manipulating micron-sized particles without mechanical contact. Moreover one can employ the RP forces to calibrate other forces in the piconewton domain. This method is termed “optical dynamometry”, and has already been used in many different situations, in Chemical Physics and in Biophysics. A few examples are quoted in ref.<sup>[6-8]</sup>, for illustration (an exhaustive list of realizations in the field would require a dedicated review). Optical dynamometry obviously demands a quantitative knowledge of the laser induced forces acting on the particle at different positions inside the beam(s). This problem was addressed theoretically in a few papers : RP forces acting on spherical particles were computed in the ray-optics approximation (ROA)<sup>[2, 6, 9]</sup>, and from generalizations of the Mie theory to Gaussian beams (GLMT)<sup>[10, 11, 12]</sup>. The

ROA can be used for various particle and beam shapes, but holds only for sizes much larger than a wavelength. The GLMT is applicable to spherical or elliptical particles, whatever the size. The main limitation of the theory lies in the representation of the laser beams in the Bromwich base of the Lorenz-Mie theory. Representing tightly focussed beams, such as those in optical tweezers, is a problem by itself [5, 13].

It is possible to experimentally measure the forces acting on a levitated or trapped particle. At equilibrium in a vertical beam, the axial force just balances the particle weight. For a spherical particle of radius  $a$  in a liquid -most often water- of viscosity  $\eta$ , the maximum transverse force,  $F_{Lmax}$ , can be estimated by flowing the liquid around the particle.  $F_{Lmax}$  is found from the minimum flow velocity to make the particle escape out of the beam,  $V$ , since  $F_{Lmax} = 6\pi\eta aV$  [14].

*Profiles* of the axial and transverse forces, i. e.  $F_{//}(e)$  and  $F_{\perp}(e)$ , where  $e$  is the distance of the particle center to the beam axis, were measured in our laboratory for polystyrene spheres in water, using a 2-parallel-beam configuration [15, 16]. Results showed a good agreement with GLMT results, except for a small systematic difference between the measured and computed values of  $e_m$ , the off-centering for which  $F_{\perp}(e)$  is maximum. We found  $[(e_m)_{GLMT} - (e_m)_{measured}]/a$  on the order of 10 %. As we suggested, this difference might be the consequence of small random excursions of the particle inside the beam, of Brownian origin or due to parasitic convection in the water [16].

RP is the mechanism that controls the equilibrium of a transparent sphere in a laser beam. Whenever the particle is made of an absorbing material, the situation is much complicated because the laser heats the particle. This heating results in convection in the surrounding fluid, which in turn produces a hydrodynamic force on the particle. Roughly, the force has a surface component and a volume one. The surface one has its origin in the non

uniform distribution of the light intensity inside the particle<sup>[17]</sup>, which in turn results in a non uniform temperature distribution on the particle surface<sup>[17, 18]</sup>. The surface temperature gradient triggers a convection of the fluid nearby and a force, generally referred to as a “radiometric” or “photophoretic” force<sup>[18]</sup>. The volume component is due to a large scale hydrodynamic instability : the heated particle plays the role of a hot point inside a fluid under gravity (see Fig.1). Such a situation, where horizontal temperature gradients are non zero, is always unstable towards convection<sup>[19, 20]</sup>. One expects a large scale flow , such as that sketched in Fig.1.

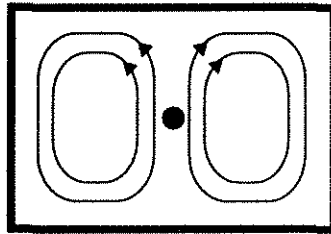


**Fig.1** : A hot particle inside a fluid bounded by a box is a source of buoyancy-driven convection. The picture is just a qualitative representation of streamlines (for small particle-fluid heat transfer rates). Exact results for the related problem of a horizontal hot wire can be found in the paper by Maquet et al.<sup>[20]</sup>.

In this paper, we want to illustrate these concepts in experiments which we carried out with moderately focussed beams, with transparent and absorbing particles. In Section 2, we briefly describe our experimental set-up and procedures. In Section 3, we show that the geometry of counter-propagating beams allows us to discriminate RP and thermal effects, a procedure that makes GLMT applicable whatever the absorption of the material constituting the particle. As we will see, thermal effects are found considerable with so-called

“superparamagnetic” particles. Conversely, they are found negligible with polystyrene particles in water, a characteristic which makes these particles appropriate for optical dynamometry experiments. An example of a recent application in this field, together with a summary of this work are given in the final Section 4.

## 2) Optical levitation

### 2.1: *Experimental procedure*

**Particles** : we used polystyrene particles (refractive index  $n = 1.59$ ) with radii ( $a$ ) in the  $6 \div 15 \mu\text{m}$  range. The particles were provided by Polysciences, as concentrated suspensions in water. Samples in optical levitation experiments were considerably diluted (in Millipore MilliQ water), in order that only one particle be trapped on the laser beam. Polystyrene is only slightly heavier than water, and its density can be precisely matched by a mixture of water and glycerol (density =  $1.261 \text{ g/cm}^3$  at  $20^\circ\text{C}$ ). Doing so, we could measure the mass density ( $\rho$ ) of the polystyrene particles within  $\pm 0.003 \text{ g/cm}^3$  for each Polysciences batch. Results vary from  $1.048$  up to  $1.056 \text{ g/cm}^3$  among the different batches.

To study the influence of particle absorption, we used so-called “superparamagnetic” beads, provided by Dynal. These are spherical particles, about  $5 \mu\text{m}$  in diameter (M-500 in Dynal’s classification), made of a dispersion of iron oxyde in a polymer. Their density (given by Dynal) is  $1.5 \text{ g/cm}^3$ . The beads are delivered as a suspension in a saline buffer, from which we made a diluted version in pure water, as for the polystyrene particles.

The particle radius value is of critical importance in the comparison of computed levitation intensities to experimental ones. We found that  $a$  is better estimated from the particle sedimentation velocity,  $V_{sed}$ , than from its microscope image.  $V_{sed}$  is given by  $6\pi\eta aV_{sed} = \tilde{m}g$ , the particle weight corrected for buoyancy. Then:

$$V_{sed} = (2/9) a^2 g \Delta\rho / \eta \quad (1)$$

where  $g$  is the gravity field and  $\Delta\rho = \rho - \rho_0$  is the particle density corrected for buoyancy ( $\rho_0$  is the water density). Doing so, we measure  $a$  essentially within half the error on  $\Delta\rho$ , i.e. about  $\pm 5\%$  for polystyrene particles.

**Set-up :** Our set-up is inspired from the design by T.Buican<sup>[21]</sup>. For a detailed description, see <sup>[15]</sup>. In the most simple situation, a single particle is manipulated by a couple of vertical, coaxial and counterpropagating Gaussian laser beams (Fig.2). The source is an Ar<sup>+</sup>

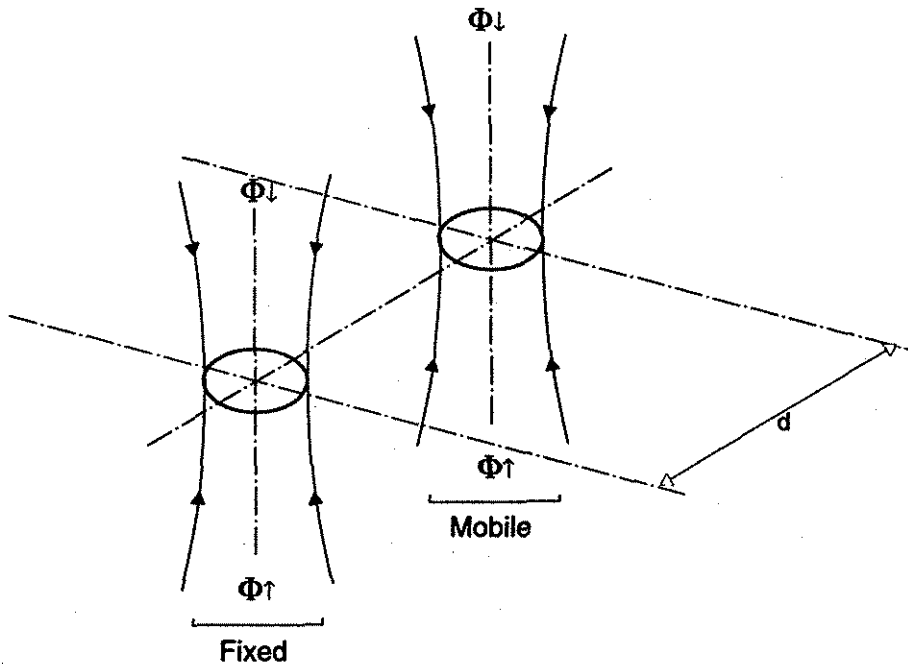


**Fig.2 :** Sketch of the optical levitation set-up beam configuration. Each levitation trap is made of a couple of counter-propagating beams. The distance ( $d$ ) between the fixed and mobile traps can be varied from 0 to about  $50 \mu\text{m}$ .

laser, operated on the 514 nm line. In the experiments of interest in this paper, the two beams are confounded, i.e. their beam-waists are located in the same horizontal plane ( $z = 0$ ). This plane is then an up-down symmetry plane. The beam-waist radius (at  $1/e^2$  of maximum intensity),  $\omega_0$ , is about 5  $\mu\text{m}$  (more accurate values are given in the examples below). We usually determine  $\omega_0$  from the far-field diffraction pattern of the beam.

The particles to be manipulated are in a water suspension, inside a glass cuvette. Polystyrene particles are more refringent than water ( $n_w = 1.34$ ) and consequently are trapped along the beam axis. In our procedure, we catch such a particle and levitate it up to the beam-waist plane. This is most simply achieved with the up-going beam ( $\uparrow$ ) only, whose power ( $\Phi_\uparrow$ ) is adjusted so as to keep the particle at  $z = 0$ . The vertical equilibrium in this plane is unstable, but only marginally. In practice, we can keep a levitated polystyrene particle at  $z = 0$  during a minute or so. The equilibrium value of  $\Phi_\uparrow$  is measured within  $\pm 1\%$ .

In the general levitation experiment, the particle is held by both up and down beams, with powers  $\Phi_\uparrow$  and  $\Phi_\downarrow$ , respectively. The two beams act uncoherently [15], consequently the RP levitation force,  $F_{RP}^{lev}$ , scales as  $\Phi_\uparrow - \Phi_\downarrow$ , while the RP transverse force (i.e. perpendicular to beam axis),  $F_{RP}^{trms}$ , scales as  $\Phi_\uparrow + \Phi_\downarrow$ .

Magnetic particles strongly absorb the green light and are repelled out of the laser beam axis. Trapping such particles needs to configurate the beams into a donut mode (see Fig.3). This may be achieved by forcing the laser to oscillate in a TEM01\* mode [1,22], or by mechanically scanning the basic TEM00 mode [23]. In our set-up, we employ a rotating tilted glass plate, as shown in Fig.3. This simple mechanism generates a tubular beam of radius  $r_0$ , with the same direction as that of the incoming Gaussian beam. The tubular shape is achieved only as an average, but the trapped particle feels it so, because the plate rotation period ( $2\pi/\Omega \approx 0.01$  s) is very small compared to  $\tau_{esc}$ , the time it takes for a particle to be expelled

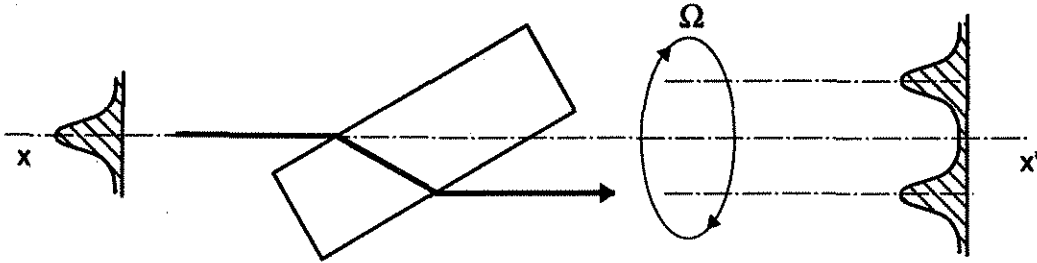


**Fig.3** : Sketch of the rotating-glass-plate device used to generate a tube of light. The plate rotates around the  $xx'$  axis. The device is located near the argon laser, in the “source” part of the set-up (see ref.[15] for details).

out of the basic Gaussian beam.  $\tau_{esc}$  is on the order of  $6\pi\eta a\omega_0 c/\Phi$ , where  $\eta$  is the water viscosity ( $\approx 0.01$  poise). In our experimental conditions,  $\tau_{esc} \approx 0.1$  sec, which makes the above mentioned condition very well satisfied.

To trap a magnetic particle on the light-tube axis, it suffices that  $r_0$  be larger than  $a$ . Levitating and equilibrating the particle at altitude  $z = 0$  then proceeds in the same way as for the transparent particles. Measuring  $r_0$  can be achieved in different ways. A simple and convenient method consists in operating the rotating plate at very slow speed (say 1 turn/minute) and trapping a polystyrene particle. The particle is trapped onto the Gaussian beam axis and follows its circular movement. The locus of particle positions is a circle, of radius  $r_0$ .

The set-up can be very easily operated in a double trap configuration, i.e. with two couples of counter-propagating beams, either in classical or tubular modes (Fig.2). The distance ( $d$ ) between the two traps can be varied between 0 and about  $50 \mu\text{m}$ . The double-beam configuration can be used to levitate a single particle (in this case  $d < 2a$ )[15] or two particles ( $d > 2a$ ).



## 2.2. RP versus hydrodynamic forces

Results of the levitation experiments are shown in Fig.4 and Fig.5 in the form  $\Phi_{\uparrow} - \Phi_{\downarrow}$  versus  $\Phi_{\uparrow} + \Phi_{\downarrow}$ , for polystyrene (Fig.4) and magnetic (Fig.5) particles. If only RP forces and gravity are acting on the particle,  $\Phi_{\uparrow} - \Phi_{\downarrow}$  is the levitation intensity,  $\Phi_{lev}$ , independently of the total power,  $\Phi_{\uparrow} + \Phi_{\downarrow}$ , illuminating the particle. A dependence of  $\Phi_{\uparrow} - \Phi_{\downarrow}$  on  $\Phi_{\uparrow} + \Phi_{\downarrow}$  is the indication that laser induced particle heating plays a role in the particle equilibrium.

Experimentally, we find that the  $(\Phi_{\uparrow} - \Phi_{\downarrow}, \Phi_{\uparrow} + \Phi_{\downarrow})$  graphs are approximately linear. The sensitivity of our method to detect particle heating is limited by the experimental error in the measurement of  $\Phi_{\uparrow}$  and  $\Phi_{\downarrow}$ , which is about  $\pm 2.5\%$ . A relative error  $\varepsilon$  in  $\Phi_{\uparrow}$  or  $\Phi_{\downarrow}$  artificially produces a slope  $\varepsilon/2$  in the graph. Consequently, only slopes greater than about 5% are meaningful for the detection of particle heating. With this criterion at hand, we may conclude that most of the polystyrene particles that we tested are transparent, i.e. negligibly absorb the laser light.

Conversely, magnetic particles (Fig.5) are much absorbant, as evidenced from the strongly negative slope of the  $(\Phi_{\uparrow} - \Phi_{\downarrow}, \Phi_{\uparrow} + \Phi_{\downarrow})$  graph (about -50%). Notice that  $\Phi_{\uparrow} - \Phi_{\downarrow}$  becomes negative beyond  $\Phi_c \approx 6.3$  mW of total power, which means that increasing the total power beyond this value reverses the sign of the apparent weight of the particle! We believe that this behavior rules out the hypothesis of radiometric forces. At  $\Phi_{\uparrow} + \Phi_{\downarrow} = \Phi_c$ , the up and down beams have the same power,  $\Phi_{\uparrow} = \Phi_{\downarrow}$ . Since the 2-beam configuration is symmetric by reflexion through the beam-waist plane, the temperature distribution throughout the particle has the same symmetry at  $\Phi_{\uparrow} + \Phi_{\downarrow} = \Phi_c$ . Consequently the radiometric forces generated by the up and down beams at  $\Phi_c$  are equal and opposite. The same property obviously holds for RP forces too. Therefore the net radiometric + RP force at  $\Phi_c$  is null. The only mechanism which can compensate for the particle weight is the gravity-driven large scale convection sketched in

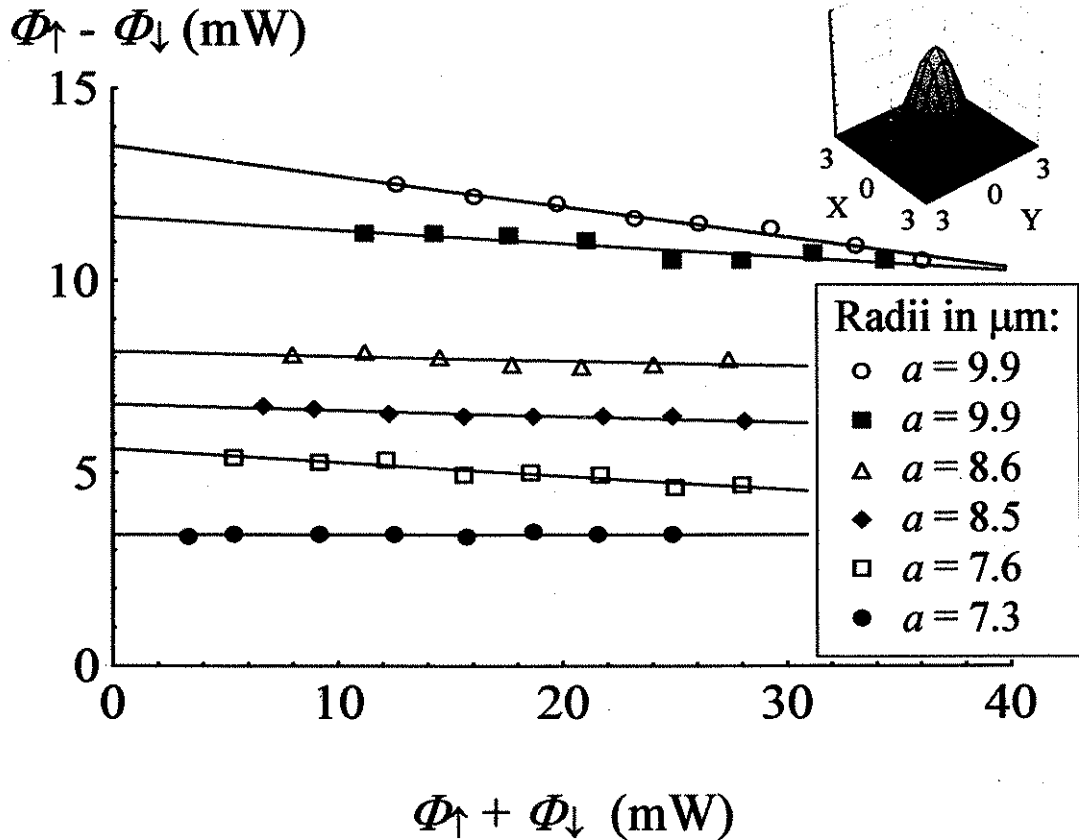


**Fig.4** : Determination of the radiation pressure levitation intensity for polystyrene spheres in water. We found horizontal graphs (within experimental error) for most of the particles. However deviations were found in a few cases, as illustrated by the top graph in the figure : here the negative slope (-7.8%) is beyond uncertainty, which means that this particle was slightly heated by the laser beams ( $\omega_0 = 4.5 \mu\text{m}$ ). The polystyrene spheres were levitated by Gaussian beams. In the perspective view of the beam structure, the beam-waist is taken as the unit length.

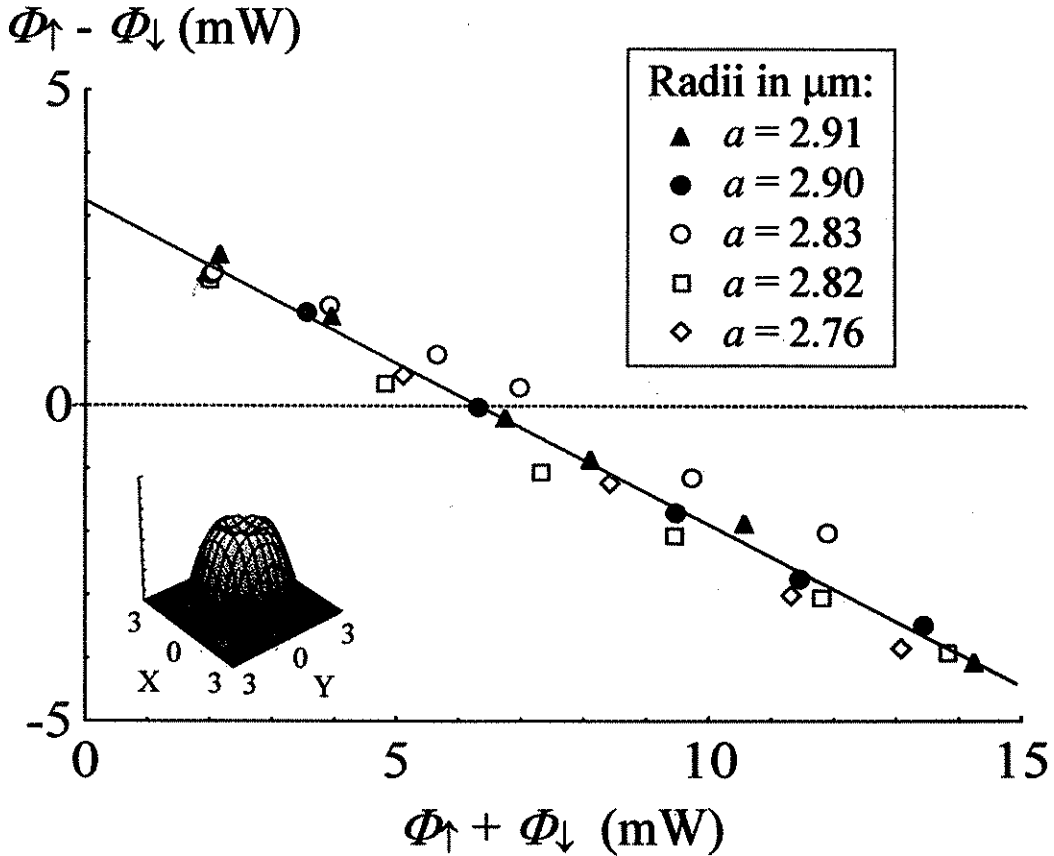


Fig.5 : Determination of the radiation pressure levitation power of magnetic particles in water. The strongly negative slope of the graph is the evidence of a considerable laser induced particle heating. These particles were levitated by tubular beams ( $\omega_0 = 5.25 \mu\text{m}$ ,  $r_0 \cong 6.2 \mu\text{m}$ ), whose structure is illustrated at the figure bottom. Extrapolating the graph to the zero-total-power limit gives  $\Phi_{RP}^{lev}$ , the RP levitation power.

Fig.1. The linearity of the  $(\Phi_{\uparrow} - \Phi_{\downarrow}, \Phi_{\uparrow} + \Phi_{\downarrow})$  graph suggests that the convection flow is simply proportional to the total power illuminating the particle. The laser-induced force acting on the particle can be represented as :

$$F = C_{RP}(\Phi_{\uparrow} - \Phi_{\downarrow}) + C_{conv}(\Phi_{\uparrow} + \Phi_{\downarrow}) \quad (2)$$

where  $C_{RP}$  and  $C_{conv}$  are constants. Eq.(2) expresses the fact that, in addition to the RP force, the particle feels a vertical hydrodynamic force,  $F_{conv}$ , whose amplitude is proportional to  $\Phi_{\uparrow} + \Phi_{\downarrow}$ . This force is produced by a flow of velocity  $V$  (far from the particle):  $F_{conv} = 6\pi\eta aV$ , with  $V$  proportional to the total power,  $\Phi = \Phi_{\uparrow} + \Phi_{\downarrow}$ . Then:

$$F_{conv} = 6\pi\eta a(\Phi_{\uparrow} + \Phi_{\downarrow}) \frac{dV}{d\Phi} \quad (3)$$

When  $\Phi = \Phi_c$ , we simply have  $C_{conv}\Phi_c = \tilde{m}g$ . With the above given definition of the sedimentation velocity (see Eq.(1)), we arrive at:

$$dV/d\Phi = V_{sed}/\Phi_c \quad (4)$$

In our experimental conditions, we find  $dV/d\Phi \cong 0.17 \mu\text{m}\cdot\text{s}^{-1}\cdot(\text{mW})^{-1}$ .

Extrapolating the experimental graphs to  $\Phi_{\uparrow} + \Phi_{\downarrow} = 0$  yields the pure RP component of the levitation force. In other words, the single beam RP levitation power,  $\Phi_{RP}^{lev}$ , is given by :

$$\Phi_{RP}^{lev} = \lim_{\Phi_{\uparrow} + \Phi_{\downarrow} \rightarrow 0} (\Phi_{\uparrow} - \Phi_{\downarrow}) \quad (5)$$

For the magnetic beads, we thus find  $\Phi_{RP}^{lev} \cong 3.2 \mu\text{W}$ . RP levitation intensities can be analyzed by means of GLMT. In Fig.6 we plotted the theoretical values of  $\Phi_{RP}^{lev}$ , computed with GLMT, for particle radii in the  $6 \div 12 \mu\text{m}$  range. Input parameters correspond to experiments with polystyrene spheres. Three curves are shown corresponding to slightly different values of the particles refractive indices. Oscillations are due to so-called "Structure resonances" (morphology dependent resonances) of the spherical particles [24, 11]. Experimental values of  $\Phi_{RP}^{lev}$  are plotted for comparison with computed ones. Error bars represent experimental

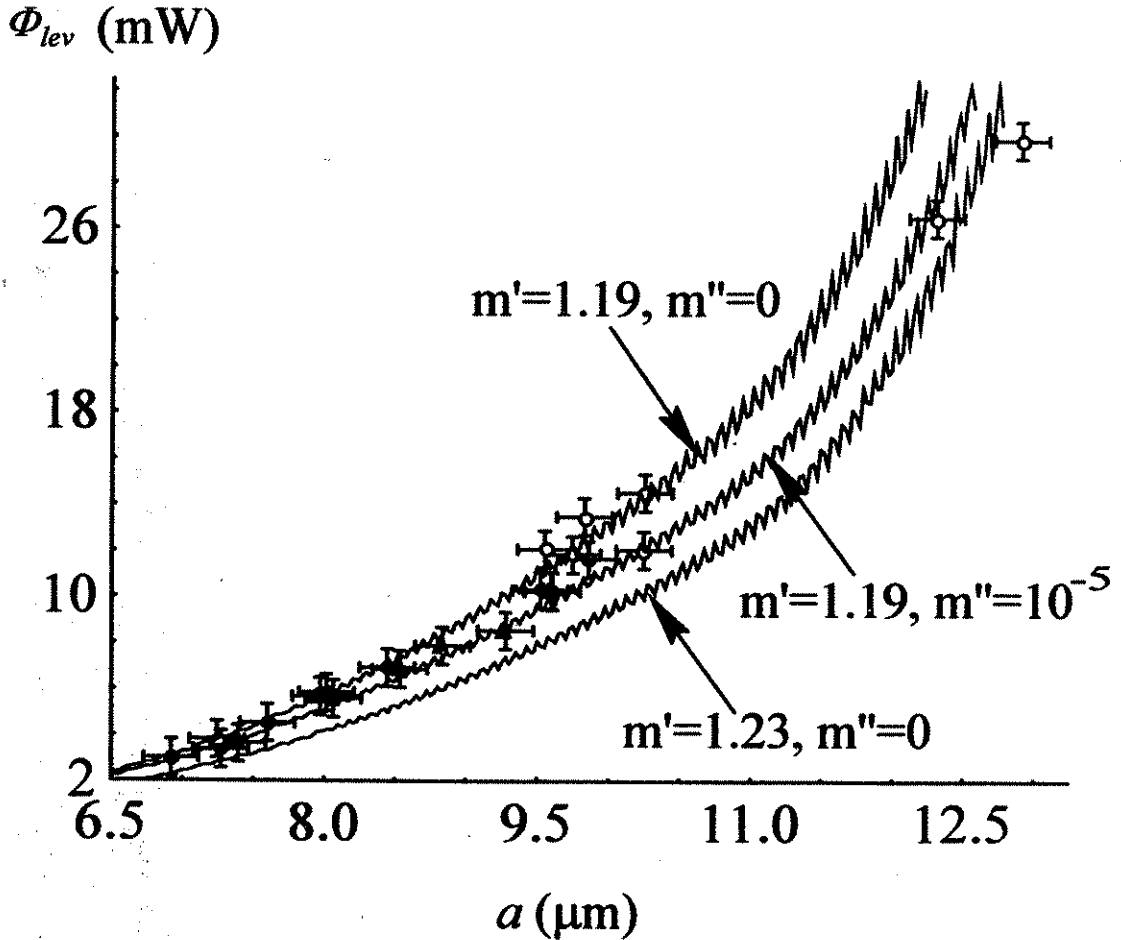


**Fig.6** : RP levitation powers of polystyrene spheres in water. Beam-waist  $\omega_0 = 4.5 \mu\text{m}$ . Experimentally measured powers are compared to those computed by GLMT, for different values of the particles complex index of refraction. Oscillations are structure resonances.

uncertainties on particle radii and extrapolated levitation intensities. In Fig.6,  $m = n/n_w = m' + im''$  is the complex refractive index of the particle relatively to that of the continuous medium (water,  $n_w \cong 1.34$  at 514.5 nm).  $m'=1.190$  corresponds to  $n=1.59$ , the

widely accepted value for polystyrene refractive index.

The ( $m'=1.19$ ,  $m''=0$ ) curve well fits to a majority of experimental points for particle radii up to about  $10\ \mu\text{m}$ . Some of the points require increased values of either  $m'$  or  $m''$ , a tendency which is most evident for the largest particles ( $a \approx 12\ \mu\text{m}$ ). This anomaly in  $m$  was already noticed prior to this work by Ashkin et al.<sup>[3]</sup>, Bakker-Schut et al.<sup>[9]</sup> and by Martinot-Lagarde et al.<sup>[16]</sup>. Since a slight laser induced heating was noticed with some of the polystyrene particles, we believe that anomalous points are due to particle absorption. Consequently, it is preferable to represent these points with  $m'=1.19$  and a non-zero value of  $m''$ . Clearly, the ( $m'=1.19$ ,  $m''=10^{-5}$ ) GLMT curve well fits to the lower part of experimental data. Notice that  $m''=10^{-5}$  corresponds to an absorption length equal to  $0.6\ \text{cm}$  for the bulk material.

Fig.7 shows the GLMT results relevant to our experiments with Dynadeads. The radius of the tubular beam was  $r_0 \cong 6.2\ \mu\text{m}$ . To compute the levitation force acting on a particle trapped on the tube axis, we may think of the system as made of a fixed Gaussian beam, of beam-waist  $\omega_0$  ( $\cong 5.25\ \mu\text{m}$  in these experiments), and of the particle rotating around the beam-axis at the distance  $r_0$ . The beam is polarized linearly in a fixed direction  $\hat{e}$ , which implies that the particle in general feels an oblique polarization state:

$$\hat{e} \cdot \hat{r}_0 = \cos \Omega t \quad (6)$$

Denoting  $F_{//}$  the levitation force when  $\hat{e} // \hat{r}_0$  and  $F_{\perp}$  that when  $\hat{e} \perp \hat{r}_0$ , we may write :

$$F(t) = F_{\perp} \sin^2(\Omega t) + F_{//} \cos^2(\Omega t) \quad (7)$$

Strictly speaking, Eq.(5) is an approximation, which amounts to supposing that the scattered fields originating from the parallel and perpendicular components of  $\hat{e}$  do not interfere. In fact, GLMT shows that they do, but only weakly. On the basis of Eq.(5), we expect the time

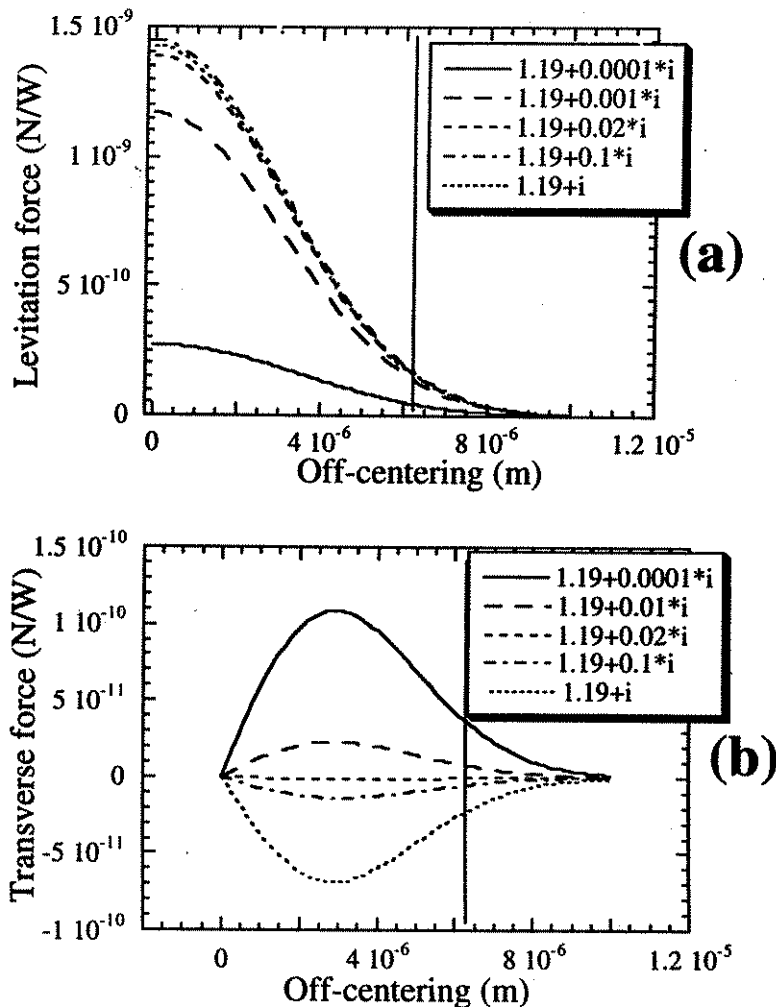


**Fig.7** : Profiles of RP forces for absorbing particles, computed by GLMT for a Gaussian beam of circular polarization. Beam-waist  $\omega_0 = 5.25 \mu\text{m}$ . The chosen particle radius corresponds to the average of measured Dynabeads radii. Symbols corresponding to different complex refractive indices are defined in each graph inset.  $r_0$  is the particle “off-centering”, namely the distance of the particle center to the beam axis. The vertical line shows the position of the particle on the axis of the tubular beam, at  $r_0 \equiv 6.2 \mu\text{m}$  from the rotating Gaussian beam axis. a) Levitation RP force ; b) Transverse (horizontal) force. Notice that the particle is expelled out of the beam for  $m'' \geq 0.02$ .

average of  $F(t)$ , i.e.  $\bar{F} = (1/2)(F_{||} + F_{\perp})$  to be the same as the force generated by a circularly polarized beam,  $F_{circ}$ . GLMT numerical results show that  $\bar{F}$  and  $F_{circ}$  differ by not more than 1%, which is an indication of the accuracy of the above approximation. The force profiles shown in Fig.7 were computed supposing a circular polarization, for 1 Watt of laser power and different values of the particle complex index of refraction. We simply supposed  $m' = 1.19$  as for pure polystyrene, and tested different values of  $m''$  in the  $10^{-5} \div 1$  range.

As Fig.7b shows, the computed radial force,  $F_{RP}^{trans}$  is positive (i.e. the particle is attracted towards the beam axis) for  $m'' \leq 0.02$  and negative for higher values. Since the particles are observed to be repelled out of the beam,  $m''$  is necessarily  $\geq 0.02$ . The experimental levitation power,  $\Phi_{RP}^{lev}$ , corresponds to 125 pN/Watt, within  $\pm 10\%$ . Computed levitation forces,  $F_{RP}^{lev}$ , are close to the experimental one for  $m'' \geq 0.02$  too and for  $r_0 \cong 6.5 \mu\text{m}$ , which is compatible with the measured off-centering, within experimental error ( $\pm 0.5 \mu\text{m}$ ). As Fig.7a shows, the  $F_{RP}^{lev}$  profiles get close to an asymptotic profile, within about 4%, for  $m'' \leq 0.02$ . Consequently, it is not possible to tell better than a lower boundary for  $m''$  from the value of the levitation power only. More information could be gained from the transverse force, which, contrary to  $F_{RP}^{lev}$ , does not saturate for high  $m''$  (see Fig.7b). Experimentally, one can extract the  $F_{RP}^{trans}$  profile from the horizontal trajectory of the particle out of the Gaussian beam axis. We will test this procedure in forthcoming experiments.

### 3. Conclusion

We carried out optical levitation experiments of micron-sized particles in water. We showed that laser induced heating of the levitated particle may greatly influence the particle equilibrium and lead to grossly wrong estimations of the radiation pressure levitation power,



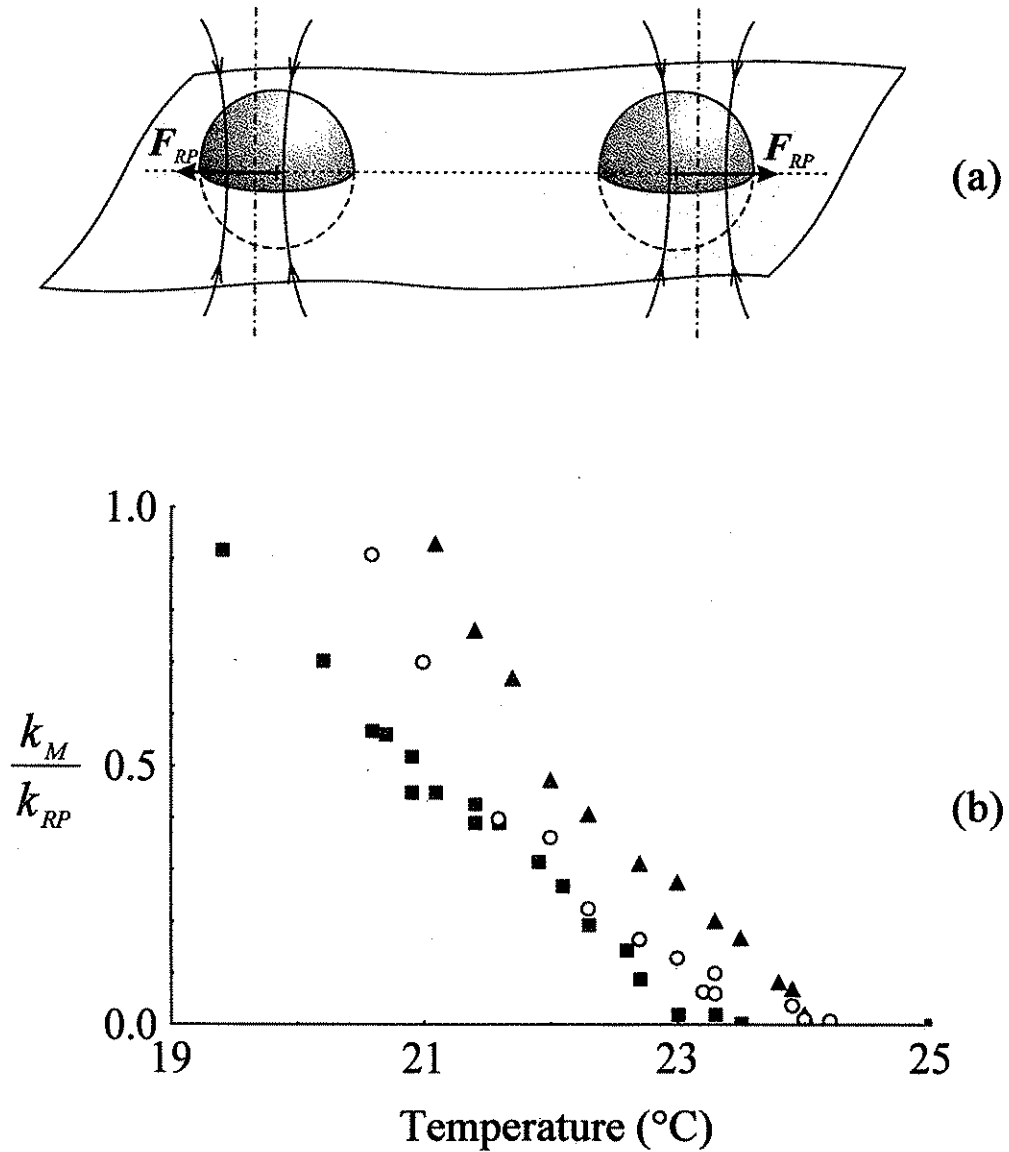


**Fig.8** : Characterization of a molecular membrane gel phase elasticity by optical dynamometry. a) Sketch of the experimental procedure with 2 polystyrene particles; b) Membrane elastic response ( $k_M$ ), as a function of temperature, up to the gel-to-fluid transition.

$\Phi_{RP}^{lev}$ . Using two vertical counter-propagating beams, we could separate hydrodynamic and RP forces and carry out a quantitative analysis of the measured levitation powers by means of GLMT. This analysis convincingly shows that thermal effects are negligible for current polystyrene microspheres in water, with moderately focussed laser beams. This conclusion qualifies such particles for optical dynamometry experiments, where it is important to rely on RP forces.

To illustrate this point with an example, we summarize in Fig.8 the principle and main result of a recent study which we carried out on the elasticity of model membranes by means of optical dynamometry. A model membrane is a single bimolecular layer made by phospholipid molecules (these are the basic constituents of cell membranes). Below a transition temperature ( $T_m$ ), such membranes form an elastic gel (much similar to an elastic rubber sheet). In our experiment, we attached 2 polystyrene particles to such a membrane and pulled them apart by means of two couples of counter-propagating beams<sup>[16]</sup>. From the displacements of both particles, and knowing the RP forces involved, we deduced a spring constant,  $k_M$ , which represents the elastic response of the gel<sup>[25]</sup>. Fig.8b shows the evolution of  $k_M$  up to the transition.  $k_M$  values are plotted in  $k_{RP}$  units: here  $k_{RP} = (dF_{RP}^{trans}/dr)_{r=0}$  represents the stiffness of the optical dynamometer. For small displacements, say  $r < 0.5a$ , the lateral radiation pressure force is proportional to  $r$  :  $F_{RP}^{trans} \propto k_{RP} \cdot r$ . In the example shown, the optical dynamometry experiment is feasible down to temperatures for which  $k_M$  becomes comparable to  $k_{RP}$ . The lateral forces in Fig.8 span a 0 to about 20 pN range, which is typical of optical dynamometry capability.

#### Acknowledgements

The authors are gratefully indebted to H.Polaert, G.Gréhan and G.Gouesbet (LESP,

INSA Rouen, France), for the kind provision of GLMT programs and fruitful discussions, and C. Dietrich for the Dynabeads sample used in the experiments. This work was supported by the Laboratoire Franco-Bulgare (CNRS/Bulgarian Academy of Sciences/University of Sofia) and by European Union, through Tempus JEP 09789.

### References

- [1] A. Ashkin, Phys. Rev. Lett. **24**, 156 (1970);  
A. Ashkin and J.M. Dziedzic, Appl. Phys. Lett. **19**, 283 (1971);  
A. Ashkin and J.M. Dziedzic, Appl. Phys. Lett. **24**, 586 (1974).
- [2] G. Roosen and C. Imbert, Phys. Lett. **59A**, 6 (1976);  
G. Roosen, Opt. Commun. **21**, 189 (1977).
- [3] A. Ashkin, J.M. Dziedzic, J.E. Bjorkholm and S. Chu, Opt. Lett. **11**, 288 (1986).
- [4] S.M. Block, "Optical tweezers" : a new tool for biophysics", in "Now invasive techniques in Cell Biology", pp 375-402 (Wiley-Liss, 1990).
- [5] K.F. Ren, G. Gréhan and G. Gouesbet, Appl. Opt. **35**, 2702 (1996).
- [6] J.Y. Walz and D.C. Prieve, Langmuir **8**, 3073 (1992).
- [7] T. Sugimoto, T. Takahashi, H. Itoh, S. Sato and A. Muramatsu, Langmuir **13**, 5528 (1997);  
Y.N. Oshima, H. Sakagami, K. Okumoto, A. Tokoyoda, T. Igarashi, K. Shintaku, S.

- Toride, H. Sekino, K.B. Kabuto and I. Nishio, *Phys. Rev. Lett.* **78**, 3963 (1997).
- [8] A. Ashkin, K. Schütze, J.M. Dziedzic, U. Euteneur and M. Schliwa, *Nature* **348**, 346 (1990);  
S.M. Block, L.S.B. Goldstein and B.J. Schnapp, *Nature* **348**, 6299 (1990);  
K. Svoboda, C.F. Schmidt, D. Branton and S.M. Block, *Biophys. J.* **63**, 784 (1992);  
S.C. Kuo and M.P. Sheetz, *Science* **260**, 232 (1993);  
S.B. Smith, Y. Cui and C. Bustamente, *Science* **271**, 795 (1996);  
K. Sakata-Sogawa, M. Kurachi, K. Sogawa, Y. Fujii-Kuriyama and H. Tashiro, *Eur. Biophys. J.* **27**, 55 (1998).
- [9] A. Ashkin, *Biophys. J.* **61**, 569 (1992);  
T.C. Bakker-Shut, G. Hesselink, B.G. de Groot and J. Greve, *Cytometry* **12**, 479 (1991);  
R. Gussgard, T. Lindmo and I. Brevik, *J. Opt. Soc. Am.* **B9**, 1092 (1992).
- [10] G. Gouesbet, B. Maheu and G. Gréhan, *J. Opt. Soc. Am.* **A5**, 1427 (1988);  
G. Gouesbet, G. Gréhan and B. Maheu, *J. Opt. Soc. Am.* **A7**, 998 (1990), 998 (1990).
- [11] K.F. Ren, G. Gréhan and G. Gouesbet, *Opt. Commun.* **108**, 434 (1994).
- [12] J.P. Barton, D.R. Alexander and S.A. Schaub, *J. Appl. Phys.* **64**, 1632 (1988) ; *ibid.* **66**, 4594 (1989).
- [13] G. Gouesbet, *Appl. Opt.* **35**, 1543 (1996).
- [14] S. Sato, M. Ohyumi, H. Shibata, H. Inaba and Y. Ogawa, *Opt. Lett.* **16**, 282 (1991).

- 
- [15] M.I. Angelova and B. Pouligny, *Pure Appl. Opt.* **2**, 261 (1993).
- [16] G. Martinot-Lagarde, B. Pouligny, M.I. Angelova, G. Gréhan and G. Gouesbet, *Pure Appl. Opt.* **4**, 571 (1995).
- [17] P.W. Dusek, M. Kerker and D.D. Cooke, *J. Opt. Soc. Am.* **69**, 55 (1979).
- [18] A.B. Pluchino, *Appl. Opt.* **22**, 103 (1983);  
S. Arnold and M. Lewittes, *J. Appl. Phys.* **53**, 5314 (1982);  
A.B. Pluchino and S. Arnold, *Opt. Lett.* **10**, 261 (1985).
- [19] E. Guyon, J.P. Hulin and L. Petit, in "*Hydrodynamique physique*" ,  
(Inter Editions/CNRS Editions, 1994).
- [20] J. Maquet, G. Gouesbet and A. Berlemont, *Int. J. Heat Mass Transfer.* **35**, 2695  
(1992).
- [21] T.N. Buican, D.L. Neagley, W.C. Morrison and B.D. Upham, in "*New Technologies in Cytometry*", SPIE Proceedings 1063, 190 (1989).
- [22] G. Roosen and C. Imbert, *Opt. Commun.* **26**, 432 (1978).
- [23] K. Sasaki, M. Koshioka, H. Misawa, N. Kitamura and H. Masuhara, *Appl. Phys. Lett.*  
**60**, 807 (1992).
- [24] R.E. Benner, P.W. Barber, J.F. Owen and R.K. Chang, *Phys. Rev. Lett.* **44**, 475  
(1980).
- [25] Proceedings of "Giant Vesicles" workshop, Ascona (1998), to be published.